A&A 508, 993–1000 (2009)
DOI: 10.1051/0004-6361/200913145

Astronomy & Astrophysics

Local re-acceleration and a modified thick target model of solar flare electrons

J. C. Brown[1], R. Turkmani[2], E. P. Kontar[1], A. L. MacKinnon[3], and L. Vlahos[4]

[1] Department of Physics & Astronomy, University of Glasgow, G12 8QQ, UK
e-mail: john@astro.gla.ac.uk
[2] Department of Physics, Imperial College, London SW7 2AZ, UK
[3] Department. of Adult and Continuing Education, University of Glasgow G12 8QQ, UK
[4] Department of Physics, University of Thessaloniki, 54006, Greece

Received 19 August 2009 / Accepted 2 October 2009

ABSTRACT

Context. The collisional thick target model (CTTM) of solar hard X-ray (HXR) bursts has become an almost "standard model" of flare impulsive phase energy transport and radiation. However, it faces various problems in the light of recent data, particularly the high electron beam density and anisotropy it involves.
Aims. We consider how photon yield per electron can be increased, and hence fast electron beam intensity requirements reduced, by local re-acceleration of fast electrons throughout the HXR source itself, after injection.
Methods. We show parametrically that, if net re-acceleration rates due to e.g. waves or local current sheet electric ($\mathcal{E}$) fields are a significant fraction of collisional loss rates, electron lifetimes, and hence the net radiative HXR output per electron can be substantially increased over the CTTM values. In this local re-acceleration thick target model (LRTTM) fast electron number requirements and anisotropy are thus reduced. One specific possible scenario involving such re-acceleration is discussed, viz, a current sheet cascade (CSC) in a randomly stressed magnetic loop.
Results. Combined MHD and test particle simulations show that local $\mathcal{E}$ fields in CSCs can efficiently accelerate electrons in the corona and and re-accelerate them after injection into the chromosphere. In this HXR source scenario, rapid synchronisation and variability of impulsive footpoint emissions can still occur since primary electron acceleration is in the high Alfvén speed corona with fast re-acceleration in chromospheric CSCs. It is also consistent with the energy-dependent time-of-flight delays in HXR features.
Conclusions. Including electron re-acceleration in the HXR source allows an LRTTM modification of the CTTM in which beam density and anisotropy are much reduced, and alleviates theoretical problems with the CTTM, while making it more compatible with radio and interplanetary electron numbers. The LRTTM is, however, different in some respects such as spatial distribution of atmospheric heating by fast electrons.

Key words. Sun: X-rays, gamma rays – Sun: flares – Sun: chromosphere – acceleration of particles

1. Basic CTTM properties and problems

Since de Jager (1964) and Arnoldy et al. (1968) the *Collisional Thick Target Model – CTTM* (Brown 1971, 1972; Hudson 1972; Brown 1973) – of flare hard X-ray (HXR) sources has become an almost *standard model* of flare impulsive phase energy transport and radiation. It offers a simple and reasonably successful description of several basic features of chromospheric HXR flares and even some aspects of the distinct coronal HXR flares (Krucker et al. 2008). These include prediction/explanation of: footpoint sources; decreasing HXR source height (e.g. Aschwanden et al. 2002; Brown et al. 2002) and source area (Kontar et al. 2008) with increasing energy; electron time-of-flight energy-dependent delays in HXR light curves (Aschwanden 2004).

However, a number of papers (e.g. Brown et al. 1990) have reviewed problematic aspects of the standard CTTM model and aspects of recent data (especially from RHESSI – Lin et al. (2002)) certainly require modification of the most basic CTTM involving a single monolithic loop. These include: the motion of HXR footpoints (Fletcher et al. 2004); the smallness of the albedo component in HXR spectra (Kontar & Brown 2006; Kašparová et al. 2007) compared to that expected from the strong downward beaming in the CTTM (Brown 1972); the relative time evolution of the heated soft X-ray (SXR) plasma emission measure $EM(t)$ and temperature $T(t)$, (e.g. Horan 1971; Stoiser et al. 2008a). In addition the difference between interplanetary and HXR source electron spectral indices is inconsistent with the CTTM prediction (Krucker et al. 2007, 2009). These suggest the need for more complex models involving e.g. dynamic filamented structures, rather than static monolithic ones. and non-collisional effects in electron transport. In terms of theory the main CTTM problems are the large fractional instantaneous density of the electron beam in the corona and the time integrated total number of electrons injected (e.g. Brown & Melrose 1977; Benka & Holman 1994; Benz & Saint-Hilaire 2003). The beam density problem has worsened as estimates of the beam (HXR footpoint) area have decreased (e.g. Fletcher & Warren 2003), though the Kontar et al. (2008) finding that the HXR source area increases rapidly with height may alleviate this. These problems arise from three factors (cf. MacKinnon 2006): (a) the high beam intensity demanded by the inefficiency of collisional bremsstrahlung compared with long range Coulomb collisional heating of the plasma. This problem is worsened (MacKinnon & Brown 1989) when additional energy *loss* processes are included such as return current

dissipation (e.g. Emslie 1981; Zharkova & Gordovskyy 2005), Langmuir wave generation (e.g. Hamilton & Petrosian 1987; Melnik et al. 1999; Kontar 2001; Kontar & Reid 2009), masering (e.g. Melrose & Dulk 1982; MacKinnon et al. 1992), electron-whistler interaction (e.g. Stepanov & Tsap 2002), Weibel instability (e.g. Karlický 2009), etc.; (b) the TTM injection assumption that no acceleration occurs in the radiation region so that each injected electron radiates only once and for a time no longer than its collisional lifetime $t_{\rm coll}$; (c) injection of the intense beam is assumed to occur from a tenuous coronal accelerator.

The term CTTM is in fact used in two different ways in the flare literature. Physically a (collisional) thick target is simply one in which the radiating electrons lose all their energy (collisonally) irrespective of geometry (Brown 1971). However, the term is often used with reference to a particular geometry (Brown 1972, 1973; Hudson 1972) where electrons are injected downward into the dense chromospheric target after acceleration in the tenuous corona. Here we will mainly address this geometry though our basic considerations of collisional and non-collisional transport are relevant to at least some of the types of coronal HXR source reviewed by Krucker et al. (2008). Our discussion also applies both to HXR footpoints of static monolithic loops and to the scenario described by Fletcher et al. (2004), where footpoint HXR sources move, probably as a result of progressive magnetic field line reconnection.

In this paper we discuss problems (a)–(c) above and propose a modified thick target scenario involving similar geometry and injection but replacing assumption (b) by a re-acceleration process acting within the HXR radiating volume. The resulting increase in electron lifetime to much greater than $t_{\rm coll}$ increases the photon yield per electron and reduces the necessary electron replenishment rate, beam density, and anisotropy.

2. HXR source requirements

2.1. Model-independent nonthermal emission measure

The instantaneous bremsstrahlung output $J(\epsilon)$ (photons s^{-1} per unit photon energy ϵ) from a source volume V, with local plasma density $n_{\rm p}(\boldsymbol{r})$, and fast electron flux spectrum $F(E,\boldsymbol{r})$ at position $\boldsymbol{r}$ and bremsstrahlung cross section $Q_{\rm B}(\epsilon,E)$ differential in ϵ is (Brown 1971)

$$J(\epsilon)=\overline{n}V\int_{\epsilon}^{\infty}\overline{F}(E)Q_{\rm B}(\epsilon,E){\rm d}E \qquad (1)$$

where the source means are $\overline{n}=\int_V n(\boldsymbol{r}){\rm d}V/V;\overline{F}(E)=\int_V n(\boldsymbol{r})F(E,\boldsymbol{r}){\rm d}V/(\overline{n}V)$. For prescribed $Q_{\rm B}$, $J(\epsilon)$ is thus related uniquely to the quantity $\overline{n}V\overline{F}(E)$ regardless of how $\overline{F}(E)$ is produced (Brown et al. 2003). The spectral shape of $J(\epsilon)$ is fixed by the shape of $\overline{F}(E)$ while the absolute scale of J is fixed by a spectrum dependent factor of order unity times $\overline{n}V\overline{F}_1$ where $\overline{F}_1=\int_{E_1}^{\infty}\overline{F}(E)$ is the total mean electron flux above some reference energy $E=E_1$. Following Brown et al. (2003), $\overline{n}V\overline{F}(E)$ is often used as the fundamental unknown "source" function in inference of HXR electron spectra from data on $J(\epsilon)$ (e.g. Piana et al. 2003; Kontar et al. 2004; Massone et al. 2004; Brown et al. 2006). An equivalent HXR source property which is more readily envisaged physically than the total $\overline{n}V\overline{F}_1$ is the total *nonthermal emission measure* of electrons of $E\geq E_1$ given by

$$EM_1=\int_V n_1(\boldsymbol{r})n(\boldsymbol{r}){\rm d}V=\overline{nn_1}V\simeq\overline{n}_1\overline{n}V \qquad (2)$$

where $n_1(\boldsymbol{r})=\int_{E_1}^{\infty}\overline{F}(E,\boldsymbol{r}){\rm d}E/v(E)$ is the local density of electrons of $E\geq E_1$. EM_1 can readily be used for example to find the mean fractional density f_1 of fast electrons if the total (thermal) emission measure $EM\simeq\overline{n}^2V$ in V is known, viz $\overline{n}_1/\overline{n}=EM_1/EM$. Note also that we can write $EM_1=\overline{n}\mathcal{N}_1$ where $\mathcal{N}_1$ is of order the total number of fast electrons in V. Numerically, in a typical large event, the necessary EM_1 is $>10^{46}$ cm^{-3} for $E_1=20$ keV so any model of an intense HXR source must involve conditions satisfying

$$EM_1=\overline{n}n_1V=f_1\overline{n^2}V=10^{47}f_1n_{10}^2V_{27}>10^{46}\ {\rm cm}^{-3} \qquad (3)$$

with $n=10^{10}n_{10}$ cm^{-3}, $V=10^{27}V_{27}$ cm^3 etc. This shows that coronal sources alone can only generate large HXR bursts if they have unusually large volume and/or density (e.g. Veronig & Brown 2004; Krucker et al. 2008). Maintenance of this EM_1 in the CTTM case requires that electrons be injected at a rate (cf. Eq. (7) below and Brown & Emslie 1988) $\mathcal{F}_1>10^{36}$ s^{-1} above 20 keV. This large value is the origin of: (i) the problematically large number of total electrons processed by the accelerator during event duration $\tau_{\rm o}$, viz. $\simeq\mathcal{F}_1\tau_{\rm o}$ or around 10^{39} in a few 100 s, equal to 100× the total electrons in a loop of $V=10^{27}$ cm^3, $\overline{n}=10^{10}$ cm^{-3}; (ii) the high beam density $n_1=\mathcal{F}_1/Av_1$ over area A. For $A=2\times10^{16}$ cm^2 (or $\simeq2''$ square) this gives $\overline{n}_1\simeq10^{10}$ cm^{-3}, a density as high as the coronal loop plasma density in which the intense CTTM beam propagates.

2.2. Electron lifetime and model-dependent replenishment rate

The instantaneous values of $\overline{n}V\overline{F}(E)$, EM_1 etc in practice change as the electrons evolve. In cases where electron lifetimes τ are short (compared to event duration or observational integration times) it is necessary to sustain $\overline{n}V\overline{F}(E),EM_1$ etc. and hence J, by maintaining the numbers of the electrons of $E\geq E_1$ at a rate given roughly by

$$\mathcal{F}_1\simeq\mathcal{N}_1/\tau=EM_1/(n\tau). \qquad (4)$$

This can be either by injection of fresh electrons from outside the HXR source to replace decaying ones (as in tbe CTTM), or by a local reaccelation process acting on those inside the source to offset their energy losses. The latter option has received very little attention in the HXR source literature and is the one we focus on in this paper. In the case of the CTTM model, maintenance of $\mathcal{N}_1$ is by replenishing injection from the corona and $\tau=\tau_{\rm CTTM}$ here is the electron collision time

$$t_{\rm coll}(E_1)=\frac{2}{n_{10}}\left(\frac{E_1}{20\ {\rm keV}}\right)^{3/2}{\rm s}=\frac{0.002}{n_{13}}\left(\frac{E_1}{20\ {\rm keV}}\right)^{3/2}. \qquad (5)$$

Since $t_{\rm coll}\propto1/n$, by Eq. (4) the injection rate $\mathcal{F}_1$ required to sustain $EM_1,\overline{F}(E)$ is independent of n (Brown 1971). If τ is reduced below $t_{\rm coll}$ by non-collisonal losses then the necessary $\mathcal{F}_1$ is increased and the problems of the CTTM worsened. Of much greater interest are situations where the lifetime τ inside the HXR source is somehow enhanced over $t_{\rm coll}$ because one can then (Eq. (4)) attain the same EM_1 for a smaller replenishment rate $\mathcal{F}_1$ but the same instantaneous total $\mathcal{N}_1$.

While increasing τ reduces $\mathcal{F}_1$ the consequences for fast electron density $\overline{n}_1$ in the source depend on the geometry of their propagation. For example, if the fast electrons were being injected into a HXR source from above, increasing τ while containing them in the same V,n (e.g. by scattering or magnetic trapping),would leave the fast electron number density unchanged

but they would last longer and sustain EM_1 for smaller $\mathcal{F}_1$. If, on the other hand, they propagated freely downward, their longer τ would cause them to penetrate more deeply, increasing the HXR source V and sustaining EM_1 with a smaller n_1 but larger V. We discuss the latter situation again in Sect. 4.

The above estimates of the necessary $\mathcal{F}_1$ etc in terms of a single τ value are only approximate. To get a more accurate picture of how electron supply requirements are modified by non-collisional energy losses and gains it is necessary to look more closely at actual photon yield and its relation to electron trajectories $E(t)$.

2.3. Electron trajectories and photon yield

In general the number $\zeta(\epsilon)$ of photons per unit ϵ emitted during the lifetime of an electron of initial energy E_* is

$$\zeta(\epsilon, E_*) = \int_{t(E\geq\epsilon)} n(\boldsymbol{r}(t))v(t)Q_{\rm B}(\epsilon, E)\mathrm{d}t, \tag{6}$$

where $n(\boldsymbol{r}(t))$ is the plasma density along the electron path, and $v(t) = (2E(t)/m_{\rm e})^{1/2}$ the electron speed while $t(E \geq \epsilon)$ is the total of all intervals during which $E(t) \geq \epsilon$. As electrons tend to decay to $E < \epsilon$ (or escape) they have to be maintained at a spectral rate $\mathcal{F}_*(E_*)$ (s^{-1} per unit E_*) to sustain the value of $\overline{n}V\overline{F}(E)$ and hence $J(\epsilon)$. $J(\epsilon)$, $\mathcal{F}_*(E_*)$ and $\overline{n}V\overline{F}(E)$ are inter-related by Brown (1971); Brown & Emslie (1988)

$$J(\epsilon) = \int_\epsilon^\infty \mathcal{F}_*(E_*)\zeta(\epsilon, E_*)\mathrm{d}E_* = \overline{n}V\int_\epsilon^\infty \overline{F}(E)Q_{\rm B}(\epsilon, E)\mathrm{d}E \tag{7}$$

where $\zeta(\epsilon, E_*)$ is now the *mean* value for a large number of electrons of the same initial $E = E_*$ since in general $E(t)$ can differ greatly between electrons of the same E_* especially in the case of stochastic acceleration – see below. (Even for purely Coulomb collisional transport there is dispersion in $E(t)$ for given E_* due to the spread in impact parameters and the finite thermal speed of target particles. Both of these are small in the CTTM and are usually neglected – Brown e.g. 1971). Clearly the $\mathcal{F}_*(E_*)$ necessary for given $J(\epsilon)$ is related to $1/\zeta$ or, crudely, to $1/\tau$ as discussed in Sect. 2.2. Note that when $\mathcal{F}_*$ varies on timescales shorter than the electron time of flight in the HXR source, Eq. (7) has to be modified to allow for energy dependent time delays between features in $\mathcal{F}_*$ and in J – i.e. acceleration and propagation effects are convoluted in time. This has been discussed in the collisional case by Emslie (1983); Aschwanden (2004). It is even more relevant to the situations discussed here which specifically involve extended electron lifetimes τ.

In the CTTM, with radiation only in the collisional propagation region (and no acceleration), the mean $\mathrm{d}E/\mathrm{d}t = \dot{E} = \dot{E}_{\rm coll} = -Knv/E$ where $K = 2\pi e^4\Lambda$ with Λ the Coulomb logarithm. The mean $E(t)$ is thus monotonic so the maximum $E = E_*$ is the initial/injection energy and we can write $\mathrm{d}t = \mathrm{d}E/(-\dot{E}) = \mathrm{d}E/|\dot{E}|$ and replace the t integration (6) by the E integration

$$\zeta_{\rm CTTM}(\epsilon, E_*) = \frac{1}{K}\int_\epsilon^{E_*} EQ_{\rm B}(\epsilon, E)\mathrm{d}E. \tag{8}$$

It is the small value of $\epsilon Q_{\rm B}(\epsilon, E)$ compared with K/E^2 here that makes collisional bremsstrahlung an inefficient source of HXRs in any model, and demands large electron injection rates and beam power. Even if we can increase the electron lifetime and reduce the necessary number supply rate *the power required is unchanged* or may even be increased.

Any non-collisional transport process which acts solely to add energy *losses* $\dot{E}$ to the collisional ones can only reduce ζ below $\zeta_{\rm CTTM}$ and so increase the necessary $\mathcal{F}_*$ and power requirements (MacKinnon 2006). The only processes capable of allowing $\zeta > \zeta_{\rm CTTM}$, hence reducing $\mathcal{F}_*$, are ones which tend on average to increase the mean electron lifetimes over $t_{\rm coll}$. (We see below that the actual effect of this on $\zeta(\epsilon)$ depends on the form of $E(t)$ and of $Q_{\rm B}(\epsilon, E)$.) Physically this corresponds to acceleration inside the HXR source, a process rather arbitrarily excluded in conventional CTTM assumptions. The effect on ζ of changing $\dot{E}$ is not immediately obvious as we show by considering some simple parametric forms $\phi(E)$ to describe the effect of the acceleration relative to collisions, viz.

$$\dot{E} = \dot{E}_{\rm noncoll} + \dot{E}_{\rm coll} = \phi(E)\dot{E}_{\rm coll}. \tag{9}$$

To measure the effect of varying ϕ on ζ we have to adopt a specific form for $Q_{\rm B}(\epsilon, E)$ and we first consider the Kramers form $Q_{\rm BK} = Q_{\rm o}/\epsilon E$ ($\epsilon \leq E$) with $Q_{\rm o}$ a constant (Kramers 1923), for which a measure of ζ is the quantity

$$\xi = \frac{K}{Q_{\rm o}}\zeta = \int_\epsilon^{E_{\rm max}} \frac{\mathrm{d}E}{\phi(E)}\,. \tag{10}$$

This simplification lets us give several illustrative analytic examples of the dependence of ζ on trajectories $E(t)$ (cf. Brown & MacKinnon 1985). The true $Q_{\rm B}$ behaves in a more complex way the consequences of which we mention below. For collisions only (CTTM), $\phi = 1$ and $\xi = E_{\rm max} - \epsilon$. Other informative cases are

- (i) $\phi(E) = 0\ \ \forall E \Rightarrow \xi \to \infty$ since the electron formally has infinite lifetime. Physically this contrived idealisation would be like dragging an electron at constant speed through the plasma, energy supply exactly offsetting losses and making $\tau \to \infty$;
- (ii) $\phi(E) =$ const. C.
  (a) $C > 0$ (net energy loss) $\Rightarrow \xi = \frac{E_{\rm o}-\epsilon}{C} = \frac{\xi_{\rm coll}}{C}$ so that ζ is only enhanced in this case for $0 < C < 1$ which is also unrealistic corresponding to to fine tuning of $\dot{E}_a$ to partially offsett losses $\dot{E}_{\rm coll}$ but not reverse them to a net gain;
  (b) $C < 0$ (net energy gain). Here $E(t)$ increases indefinitely ($E_{\rm max} \to \infty$), as $t \to \infty$ and $\xi = (E_{\rm max} - \epsilon)/|C| \to \infty$. Though an infinite lifetime is clearly unphysical, arbitrarily increased ζ is possible if arbitrarily high $E_{\rm max}$ is reached;
- (iii) $\phi(E) = -\phi_1(E/E_1)^a$ with $\phi_1 > 0$ (net energy gain). Here again there is a formally infinite lifetime with $E_{\rm max} \to \infty$ as $t \to \infty$ but, for $a \neq 1$,

$$\xi = \frac{E_1}{(a-1)\phi_1}\left|\left(\frac{\epsilon}{E_1}\right)^{-a+1} - \left(\frac{E_{\rm max}}{E_1}\right)^{-a+1}\right|. \tag{11}$$

  This diverges for $a \leq 1$ but is finite $\forall a > 1$ despite the infinite lifetime ($E_{\rm max} \to \infty$). This is because $Q_{\rm BK} \propto 1/E$, with maximum value at $E = \epsilon$ so that the contribution to ξ falls as E increases and the total is finite for any sufficiently fast acceleration ($a > 1$).

These examples show how ζ can depend on the specific form of the electron trajectory $E(t)$. In addition, ζ depends on the form of $Q_{\rm B}$ in relation to $E(t)$. For any ϵ, ζ will be largest when $E(t)$ maximises the time spent near the value of E where $Q_{\rm B}$ peaks. For the Kramers $Q_{\rm BK}$ used above this is at $E = \epsilon$ but even for the next simplest approximation – the non-relativistic Bethe Heitler form $Q_{\rm BBH}$ – the peak is substantially shifted to $E \approx 1.7\epsilon$ as is

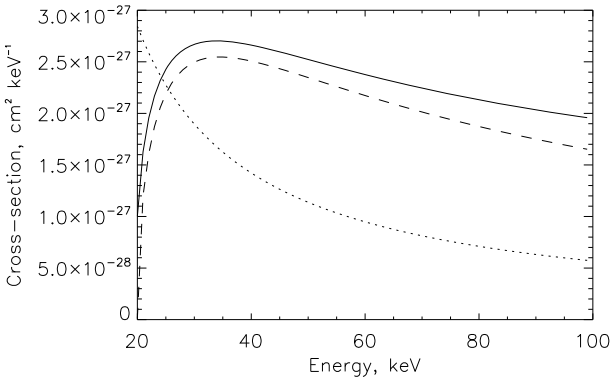

Fig. 1. Cross section $Q_B(\epsilon, E)$ at $\epsilon = 20$ keV showing how the emission contribution per unit ϵ peaks at different E for different Q_B. (Dotted = Kramers, dashed = Bethe Heitler, solid = exact (Haug 1997)).

also the case for the full cross section as given by Haug (1997) – see Fig. 1. Different forms of $E(t)$ convolved with these Q_B can result in substantial differences in rates of emission and hence in ζ.

These special cases illustrate how ζ can be enhanced by re-acceleration $\dot{E}_a$ either by making the net loss rate $|\dot{E}| < |\dot{E}_{\rm coll}|$ or by creating a net gain rate so that $E_{\rm max} > E_*$, both increasing the electron lifetime at $E > \epsilon$. This reduces the necessary injected beam density and total numbers of electrons by prolonged re-acceleration of them in the HXR source after injection. We call this the local re-acceleration thick target model (LRTTM). In Sect. 3 we discuss a specific physical energy release scenario where these LRTTM requirements may be met. We emphasize again that reducing $\mathcal{F}_1$ in this way does not reduce the power that has to be delivered. This is always at least the value in the CTTM since, for every erg of collisional bremsstrahlung emitted, of order 10^5 erg go into long range collisional energy losses. However, in the LRTTM, most of that power is delivered in the HXR source rather than in an external accelerator/injector of electrons as in the CTTM case, a point to which we return in Sect. 4.

To see whether and to what extent this happens in any particular LR scenario we have to recognise that the actual photon yield $\zeta(\epsilon)$ during the lifetime of an electron in such scenarios is more complicated than discussed above. The t integral in Eq. (6) cannot be written simply as an integral over E, as it can in these cases, since:

1. $E(t)$ is no longer monotonic in general, with $\dot{E}$ taking values >0, <0, or 0 at different parts of its path. Then the t integral can only be written as a sum of E integrals with one for each t segment in which $E(t)$ is monotonic (with $\dot{E} > 0$ or $\dot{E} < 0$) plus integrals over t itself when $\dot{E} = 0$ so that dt does not transform to a finite dE. In practice one reverts to the basic t integration (6);
2. even if the change in variable from t to E is useful, the upper limit in the E integrals is no longer the initial energy E_* (as it is in the CTTM) but the maximum value $E_{\rm max}(E_*)$ reached during the electron lifetime at $E \geq \epsilon$;
3. in re-acceleration, e.g. by waves, the trajectories $E(t)$ are not only non-monotonic but may well be highly stochastic, differing between electrons of the same initial E_* (cf. Sect. 3 for a specific example). There is then no well defined deterministic yield $\zeta(\epsilon, E_*)$ for electrons of initial $E = E_*$ and the total yield has to be found numerically by evaluating expression (6) for each electron and summing them, or using statistical techniques (e.g. Bian & Browning 2008).

3. Current sheet cascades (CSCs) as one possible LRTTM scenario

The LRTTM idea that local reacceleration of electrons inside the thick target HXR source can greatly increase their photon yield by prolonging their lifetimes to $\gg t_{\rm coll}$ is a quite general one which might be realized for many different (re)acceleration mechanisms. The basic requirement is some source of strong electric fields distributed through the source and this might be achievable in a variety of ways – e.g. Lionello et al. (1998), Fletcher & Hudson (2008). In this section we focus on one possibility to illustrate the idea in some detail.

3.1. Energy release and electron acceleration in CSCs

The CTTM idea of separation of the acceleration and radiation volumes had its origins partly in the ideas that : energy is most easily stored in the corona (Sweet 1958); acceleration is more efficient in a tenuous collisionless volume (e.g. Hamilton & Petrosian 1992; Miller et al. 1997), while bremsstrahlung gives most volumetric yield at high densities. In such cases, magnetic energy release is assumed to be driven by organized and continuous twist or shear of large scale magnetic structures (isolated loops or arcades) – e.g. Forbes & Priest (1995). An alternative is distributed small scale release of energy in a current sheet cascade (CSC) (Galsgaard & Nordlund 1997; Galsgaard 2002), resulting from the 3-D MHD response of a loop to a random underlying photospheric driver. This gives a specific physics-motivated example of the type of local re-acceleration scenario discussed schematically in Sect. 2. After a few Alfvén times (secs), Lorentz forces create stresses along the entire loop and form a hierarchy of reconnecting current sheets, leading to plasma jets. These perturb the neighboring plasma and eventually create a turbulent CSC throughout the volume from large scale current sheets (CSs) to numerous small scale CSs in which energy is dissipated randomly everywhere. CSs appear and disappear over short times but with an overall quasi-steady turbulent state. This energy release and acceleration process operates not only in the corona but also in the chromosphere (e.g. Daughton et al. 2008). Several papers have discussed particle acceleration in the CSC electric fields $\mathcal{E}$ in such a dynamic environment (Anastasiadis & Vlahos 1994; Dmitruk et al. 2003; Arzner & Vlahos 2004; Vlahos & Georgoulis 2004; Vlahos et al. 2004; Turkmani et al. 2005, 2006), the last two of which simulated particle acceleration in the $\mathcal{E}$ fields present in the coronal case of such models. For the present paper we conducted similar calculations for already energetic electrons injected into the dense chromospheric part of the loop. Trajectories $E(t)$ of test particles, with prescribed initial energy E_* randomly injected in space, were traced in a frozen "snapshot" of the MHD fields since acceleration times ($\ll$1 s) are much shorter than the overall MHD evolution timescale (~seconds). Electrons gain or lose energy stochastically as they travel along guide fields and pass through the local CS $\mathcal{E}$-fields and lose it collisionally, following complicated trajectories as they receive kicks of various signs and strengths. Some test electrons encounter few or no CSs and decay purely collisionally, rejoining the local thermal plasma.

Following Turkmani et al. (2005, 2006) we found that, in the corona, strong acceleration of a substantial fraction of thermal electrons occurs for reasonable values of the resistivity η so long as super-Dreicer $\mathcal{E}$ occur in some of the current sheets. In common with most acceleration modelling, it is hard to assess realistically how high this fraction is in a test particle approach involving scaled numerical resistivity and resolution. If the fraction

becomes very high (as it has to in the CTTM to create enough HXRs) the validity of the MHD/test particle approach becomes questionable since the associated currents should be allowed to feed back on the MHD field equations. As we show below, in the LRTTM, the necessary $\mathcal{F}$ is reduced, which alleviates this issue. Our goal here is simply to show the implications for HXR source requirements if extensive re-acceleration *does* occur.

After undergoing acceleration in the corona, electrons mainly precipitate into the chromosphere where many of them, instead of rapid collisional decay, undergo re-acceleration in the chromospheric CS $\mathcal{E}$ fields. In this paper we therefore only discuss what happens to these electrons once injected into the chromosphere, namely a substantial fraction of them survives at high energies for many collision times, increasing the photon yield ζ over the purely collisional CTTM value. This is a good example of the type of LR scenario suggested schematically in Sect. 2 since the CTTM distinction between acceleration and radiation regions disappears, and (re-)acceleration occurs in the HXR source.

3.2. CSC simulations of electron (re)-acceleration

For the coronal part of the loop we adopted plasma values $n = 10^{10}$ cm^{-3}, $T = 10^6$ K, $B = 10^2$ G and for the chromospheric part $n = 10^{13}$ cm^{-3}, $T = 10^4$ K, $B = 10^3$ G, though we recognise that these vary in space (especially n in the chromosphere). The depth of the chromosphere is taken to be 7.5×10^3 km. Here we neglect the effects of neutrals since at $T = 10^4$ K the chromospheric plasma is nearly full ionized. Future LRTTM modeling with more realistic treatment of spatial structure should include the effect of neutrals in deeper cooler regions such as modifying the resistivity and the collision rate. Collisions were treated using a modified form of $\dot{E}$ with the form $\dot{v}/v \propto v^{-3}$,valid for $v \gg v_{\rm th}$, multiplied by the factor $v^3/(v + v_{\rm th})^3$ to avoid incorrect divergence near thermal speeds $v \simeq v_{\rm th}$.

In the corona, after undergoing numerous CS $\mathcal{E}$-field accelerations and decelerations, and collisions (Turkmani et al. 2005, 2006) many coronal electrons escaped to the chromosphere, a situation geometrically similar to the injection assumed in the CTTM with little collisonal HXR emission in the tenuous corona. However, once in the chromosphere, as well as collisions, electrons now undergo re-acceleration by the CS $\mathcal{E}$ fields there. This greatly extends some of their lifetimes beyond $t_{\rm coll}$, increasing the mean photon yield ζ and reducing the replenishment rate $\mathcal{F}_1$ hence the beam density $\mathcal{F}_1/Av_1$ needed over area A to provide the HXR output J, and so alleviating the problem of their large values in the CTTM. In practice the corona accelerates and injects electrons with a spectrum of E_* – roughly a double power law distribution function (Turkmani et al. 2005, 2006). Simulations of these spectral characteristics of injected electrons and the resulting bremsstrahlung spectra arising from the complex distribution of trajectories $E(E_*, t)$ in the thick target with re-acceleration (LRTTM) will be the subject of future work. Here, to be able to compare simply the dynamics and photon yields of electrons arriving in the chromosphere for CTTM and LRTTM cases, we limit our analysis to an ensemble of electrons all of the same E_*.

We have carried out such simulations of $E(t)$ for 10^3 electrons injected randomly with $E_* = 50$ keV in a chromospheric CSC plasma with $\mathcal{E}, B$ fields from the MHD simulations discussed in Sect. 3.1 and also for the purely collisonal case. In some simulations, chromospheric CS $\mathcal{E}$ values were high enough for some electrons in the tail of the local thermal distribution to be accelerated but we do not consider these further here. The simulation results depend on the electric field which can vary from one snapshot to another according to the dynamics of the turbulent loop. The main features of our simulations are as follows:

1. *The accelerating electric field*: in the context of particle acceleration, electric fields are often compared with the Dreicer Field $\mathcal{E}_D$ (required for the force $e\mathcal{E}_D$ to overcome collisions for a thermal electron of $E \simeq kT$). Fast electrons arriving from the corona already have $E \gg kT$ in the chromosphere and the field required for re-acceleration to overcome collisions for them is smaller than $\mathcal{E}_D$ by a factor kT/E.
2. *The values of electric fields*: the electric fields are zero outside the current sheets and found to take random values inside them. The average of this value in the illustrative case used in this paper is $\mathcal{E} = 8.2 \times 10^{-4}$ statvolt/cm in the chromosphere and its maximum value is $\mathcal{E}_{\rm max} = 2 \times 10^{-2}$ statvolt/cm. The thickness of the current sheets vary between a minimum of 0.5 km and a maximum of 12.5 km. However, comparison of cases in terms of "average" $\mathcal{E}$ values is not very meaningful. One could for example have two cases with the same volume-averaged $\mathcal{E}$ in one of which $\mathcal{E}$ nowhere approached $\mathcal{E}_D$ while in the other $\mathcal{E}$ exceeded $\mathcal{E}_D$ in some local CSs. Differences in the values of $\mathcal{E}$ affect the fraction of the injected electrons undergoing re-acceleration, before being lost by escape or collisions. They also affect the maximum energies electrons reach and their lifetimes.
3. *Direction of the fields*: since the electrons encounter CS $\mathcal{E}$ fields in quasi-random directions, the electrons move back and forth on guide B fields and their acceleration is stochastic with $\dot{E}$ undergoing many changes of sign (cf. Sect. 2.3) as shown in Fig. 2a. Though the electric fields are often high enough to accelerate or decelerate the electrons inside the CSs, there is no global runaway because of the short durations and quasi-random signs of these kicks. Scattering of the electrons also helps enhance their lifetimes by keeping them in the CSC region.
4. *Numerical Resistivity and Resolution*: the electric field considered here is the resistive electric field parallel component and its value depends on the resistivity. The average numerical resistivity used here inside a chromospheric CS was taken to be $\eta = 3 \times 10^{-13}$ s (roughly the Spitzer value) and, when combined with the numerical resolution used in our simulation, results in re-acceleration of electrons in the keV−MeV range most relevant to HXR burst production. Higher (anomalous) resistivities enhance the re-acceleration process. Increasing the resolution of the numerical 3D MHD experiment leads to more and thinner fragmented CSs. This enhances the re-acceleration process since the electrons undergo a higher number of smaller kicks, and pass more often through electric field free zones in between.

We found that, in the chromosphere, among the 10^3 test electron CSC cases we ran, about 65% of injected 50 keV electrons underwent varying amounts of re-acceleration and lifetime enhancement well beyond the collision time $t_{\rm coll} = 3.2 \times 10^{-3}$ s. Some examples of these re-accelerated electron trajectories $E(E_*, t)$ are shown in Fig. 2a for nine chromospherically re-accelerated electrons and for a CTTM electron. It can be seen that electrons initially gain and lose energy in the CSs they randomly pass through, eventually entering electric field free zones where they escape or lose their energy to collisions. For our parameters, the increase in lifetimes of the injected electrons over $t_{\rm coll}$ ranged from factors slightly higher than unity to around 20× with an average over all electrons of about 5×.

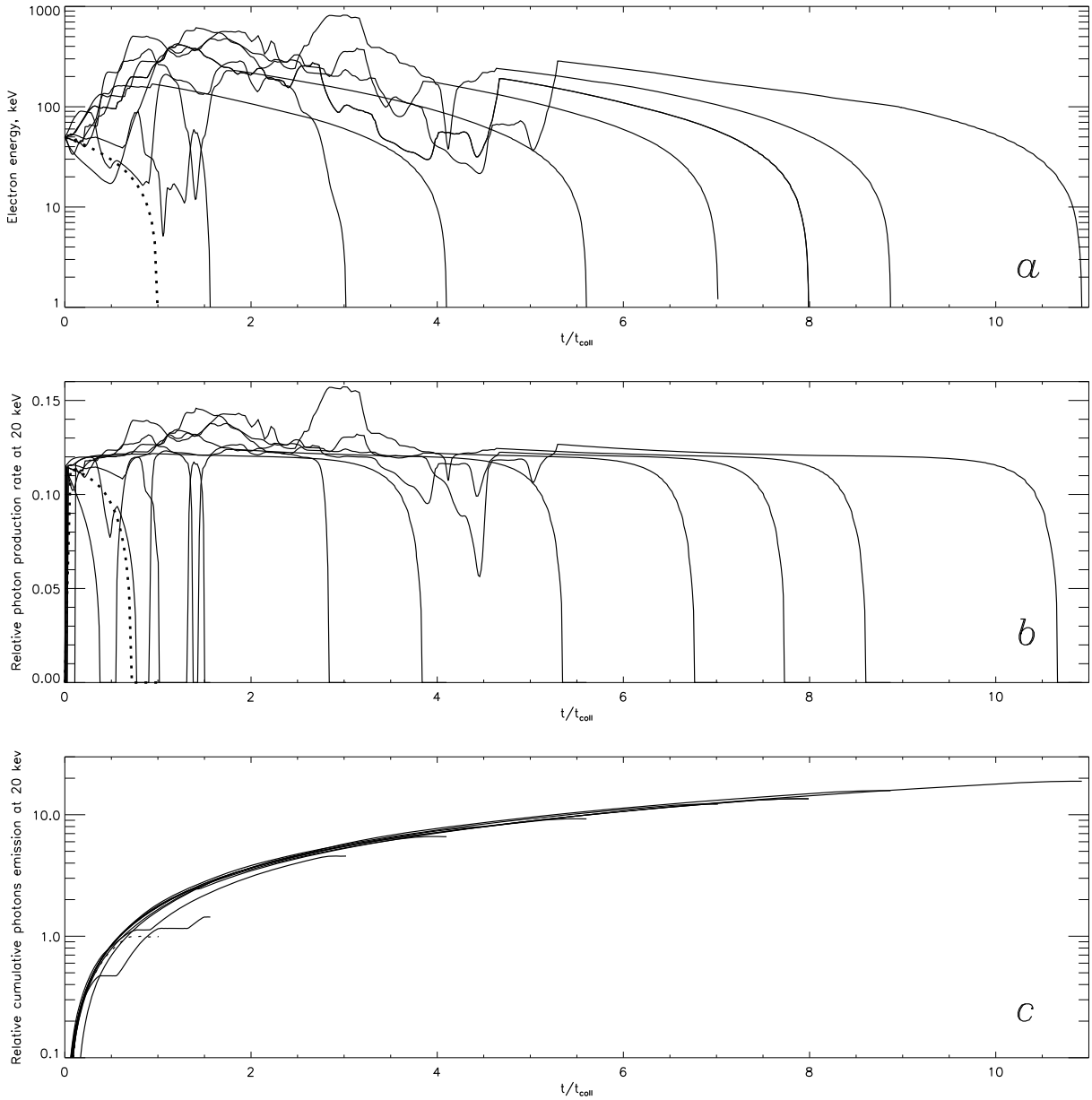

Fig. 2. Panel **a)**. Examples of trajectories $E(E_*, t)$ for nine electrons re-accelerated in the chromosphere. and one (dotted curve) undergoing collisional losses only, after arriving from the corona with initial energy $E_* = 50$ keV. Panel **b)**. Relative photon production rate at 20 keV. Panel **c)**. Relative cumulative photon production $\int_0^t \dot{\zeta}(\epsilon, t)\mathrm{d}t$ keV^{-1} at $\epsilon = 20$ keV for electrons shown in Panel a. Time is in units of the collision time for a 50 keV electron ($t_{\rm coll} = 0.0032$) s. The emission rates in b. and total emissions in **c)** have been divided by the total yield $\zeta_{\rm CTTM}$ keV^{-1} at 20 keV of a purely collisional electron starting at $E_* = 50$ keV. In **c)**, the $\zeta(t)$ curves that stop at some t have attained their asymptotic values there, the electron $E(t)$ having dropped below 20 keV thereafter.

3.3. Numerical results for photon yield ζ in the CSC LRTTM

As noted in Sect. 2.3, in the LRTTM scenario, electron trajectories $E(E_*, t)$ starting from energy E_* are not deterministic but stochastic. Thus the only way to arrive at a measure of the photon yield $\zeta(\epsilon, E_*)$ for a single test particle is to use its individual equation of motion to compute $E(t)$ for use in time integration (6). This is repeated for each of a sample of electrons initially of the same energy E_* but randomly located then undergoing random kicks in the stochastic $\mathcal{E}$ fields. We want to compare the mean $\zeta(\epsilon, E_*)$ of these with the CTTM value $\zeta_{\rm CTTM}(\epsilon, E_*)$. In the CTTM an electron injected with $E_* \le \epsilon$ yields no photons of energy $>\epsilon$ since $\dot{E}_{\rm coll} < 0$. This is not true in the presence of re-acceleration since $E_{\rm max}$ can exceed E_*. Some criterion therefore has to be adopted for comparison of photon yields. Here we chose conservatively to compare the average photon yields $\zeta(\epsilon, E_*)$ for the CTTM and CSC for electrons launched inside the source from a specified initial high energy $E_* > \epsilon$ namely 50 keV.

Based on Eq. (6) we calculated for each test electron, using the accurate form of $Q_{\rm B}$ from Haug (1997)the rate $\dot{\zeta}$ of emission of photons per unit ϵ at 20 keV as a function of t for each electron and also the cumulative number emitted up till t per unit ϵ as a function of t, hence the total ($t \to \infty$) ζ value for each electron – see Figs. 2b, c. In the unique CTTM case (Eq. (6)) for $E_* = 50$ keV $\zeta_{\rm CTTM}(\epsilon, E_*) \approx 2.2 \times 10^{-4}$ photons per keV at $\epsilon = 20$ keV. The resulting mean increase in total photon yield per keV at 20 keV reached as high as a factor of around 20 with

an average value around 10. These factors are higher than the increases in electron lifetimes mentioned above for the reason discussed in Sect. 2.3. For the given E_* the resulting increase in yield $\zeta_{\rm CSC}(\epsilon, E_*)$ compared to the collisional case increases with ϵ. As we allow $\epsilon = 10, 20, 30, 40, 45, 49$ keV to approach E_* the relative increase factors $\zeta_{\rm CSC}/\zeta_{\rm CTTM}$ in average yield were about 5, 10, 15, 50, 100, 800. This is because, in contrast with the monotonic CCTM fall of $E(t)$ from E_*, in the LRTTM many electrons of initial $E = E_*$ spend many times $t_{\rm coll}$ at $E \gg E_*$, e.g. 50−800 keV in the example shown in Fig. 2. This produces many times more photons not only at 20 keV, as discussed above, but also at much higher ϵ whereas in the CTTM there is no photon yield above 50 keV. A proper comparison of LRTTM yield with CTTM is thus rather complicated and will require numerical simulations for many E_* and ϵ values. But it is clear that the factors quoted above for the LRTTM photon yield enhancement are conservative lower limits.

4. Discussion and conclusions

We have shown that substantial re-acceleration in the chromosphere of electrons accelerated in and injected from the corona can greatly reduce the density and number of fast electrons needed to produce a HXR burst, and how this might occur in a CSC as one example. In the LRTTM. as in the CTTM, most electron collisions are in the chromosphere so the LRTTM also predicts HXR footpoints. Some of its other properties are, however, quite distinct and need much more quantitative work beyond our outline ideas above for the model to be evaluated and tested. Here we conclude by briefly discussing some of the issues to be addressed.

1. *Fast electron anisotropy.* In our CSC simulations we find that the electrons move more or less equally up and down the loop axis ($\langle v_{z+}\rangle \simeq \langle v_{Z-}\rangle$) with $\langle v_\perp\rangle/\langle v_\parallel\rangle$ about 0.05 in the chromosphere and 0.20 in the corona. Unlike the strong downward beaming ($\langle v_{z+}\rangle \gg \langle v_{z-}\rangle$) in the basic CTTM (Brown 1972), this distribution is broadly consistent with (Kontar & Brown 2006) albedo mirror diagnostic "near isotropy" results from RHESSI spectra. The $v_\perp/v_\parallel \ll 1$ property of electrons in the CSC LRTTM may, however, still yield enough H_α impact polarization to contribute to that observed (Henoux & Chambe 1990; Kašparová et al. 2005) though other mechanisms (e.g. fast proton impacts) may also contribute (Henoux et al. 1990).
2. *HXR fine time structure and footpoint synchronism.* When fast electrons in the chromospheric HXR source originate by injection from the corona, the HXR light curve should reflect the coronal supply rate quite closely since even the LRTTM extended fast electron lifetimes τ are short. So this scenario is consistent with HXR fine time structure (<1) s (Kiplinger et al. 1983), footpoint synchronism findings (Sakao et al. 1996), and energy-dependent time-of-flight delay results (Aschwanden 2004), provided that acceleration in the coronal CSCs is coherent on short enough timescales. This coherence should be on the coronal loop Alfvén timescale $\tau_{\rm A} \simeq L/v_{\rm A} \simeq 0.5 L_9 n_{10}^{1/2}/B_3$ so $B \simeq 500$ Gauss suffices to make $\tau_{\rm A} < 1$ s.
3. *Interplanetary and HXR flare electron fluxes and spectra.* In the CTTM the power law spectral index γ of HXR emission $J(\epsilon)$ is related to the spectral index $\delta_{\rm thick}$ of the electron injection rate $\mathcal{F}(E_{\rm o})$ by $\gamma = \delta_{\rm thick} - 1$ and to the mean source electron flux $\overline{F}(E)$ index $\delta_{\rm thin}$ by $\gamma = \delta_{\rm thin} + 1$. ($\delta_{\rm thick} - \delta_{\rm thin} = 2$ because the collisonal energy loss cross section varies as E^{-2}). In the LRTTM situation trajectories $E(t)$ are stochastic and average behaviour depends on the specific CSC realisation so no such obvious simple relationship exists. This complication also means that while integral deconvolution of $J(\epsilon)$ (e.g. Brown 1971; Brown et al. 2006) to find the HXR source $\overline{n}\overline{V}\overline{F}(E)$ is still fully valid, inference of $\mathcal{F}_*(E_*)$ is much more difficult because of the stochastic character of the electron transport, in contrast with the simple CTTM collisional case.
Using RHESSI and WIND data, Krucker et al. (2007) studied the relationship of electron spectra and numbers at the Sun to those near the Earth above 50 keV. They find the indices and numbers to be well correlated in all events involving free streaming from the Sun but that the relationship of spectral indices does not match the CTTM prediction (Krucker et al. 2007, 2009). Further, the numbers of electrons in IP space and in Type III Bursts are smaller by a factor of order 500 (Krucker et al. 2007) than required for the HXR source in the CTTM model. The numbers required for microwave bursts are also often found to be considerably less than for HXRs in the CTTM interpretation though this number is very sensitive to assumed conditions Lee & Gary (2000). For these to be consistent with the LRTTM reduction in electron numbers would imply even more effective re-acceleration than in the illustrative example we gave here, such as due to anomalous resistivity.
4. *Impulsive flare heating.* Various aspects of impulsive flare heating data have been invoked in support of the CTTM, including the Neupert Effect that flare soft XR light curves correlate with the integral of HXR light curves (Neupert 1968). This is often attributed to CTTM collisional heating of the SXR source plasma by HXR emitting fast electrons. However, the observed relative time sequences of $EM(t), T(t)$ are hard to reconcile with this in any obvious way even when filamented loop structures are considered (Veronig et al. 2005; Stoiser et al. 2008b). In the LRTTM the total power delivered to fast electrons in order to offset collisional losses is comparable to that in the CTTM model and can likewise heat the impulsive flare atmosphere, though the spatial distribution of that heating can be very different from the CTTM case. In the proposed LRTTM scenario the coronally injected beam rate $\mathcal{F}_1$ is reduced considerably from the CTTM rate so beam heating of the corona is reduced from its CTTM value. However, for given HXR output, the total beam power involved in the whole HXR source has to be at least as large as in the CTMM. Thus in the LRTTM more power goes into chromospheric heating as re-acceleration drives fast electrons against collisional losses there. In addition, if the extended electron lifetimes result in their penetrating deeper, beam heating may be effective to much greater depths than in the CTTM. This might offer a solution to the problem of heating white light flares by electron beams (Neidig 1989; Fletcher et al. 2007).

Acknowledgements. We gratefully acknowledge financial support of this work by a UK STFC Rolling Grant (J.C.B., E.P.K., A.L.M.) and Advanced Fellowship (E.P.K.), an EU Training Network (L.V.), a Royal Society Dorothy Hodgkin Fellowship (R.T.), ISSI Bern (J.C.B., E.P.K., L.V.) and the Leverhulme Trust (E.P.K.).

References

Anastasiadis, A., & Vlahos, L. 1994, ApJ, 428, 819
Arnoldy, R. L., Kane, S. R., & Winckler, J. R. 1968, ApJ, 151, 711
Arzner, K., & Vlahos, L. 2004, ApJ, 605, L69
Aschwanden, M. J. 2004, ApJ, 608, 554
Aschwanden, M. J., Brown, J. C., & Kontar, E. P. 2002, Sol. Phys., 210, 383

Benka, S. G., & Holman, G. D. 1994, ApJ, 435, 469
Benz, A. O., & Saint-Hilaire, P. 2003, Adv. Space Res., 32, 2415
Bian, N. H., & Browning, P. K. 2008, ApJ, 687, L111
Brown, J. C. 1971, Sol. Phys., 18, 489
Brown, J. C. 1972, Sol. Phys., 26, 441
Brown, J. C. 1973, Sol. Phys., 28, 151
Brown, J. C., & Emslie, A. G. 1988, ApJ, 331, 554
Brown, J. C., & MacKinnon, A. L. 1985, ApJ, 292, L31
Brown, J. C., & Melrose, D. B. 1977, Sol. Phys., 52, 117
Brown, J. C., Karlicky, M., MacKinnon, A. L., & van den Oord, G. H. J. 1990, ApJS, 73, 343
Brown, J. C., Aschwanden, M. J., & Kontar, E. P. 2002, Sol. Phys., 210, 373
Brown, J. C., Emslie, A. G., & Kontar, E. P. 2003, ApJ, 595, L115
Brown, J. C., Emslie, A. G., Holman, G. D., et al. 2006, ApJ, 643, 523
Daughton, W., Roytershteyn, V., Albright, B. J., et al. 2008, AGU Fall Meeting Abstracts, A1705
de Jager, C. 1964, in Research in Geophysics, Sun, Upper Atmosphere, and Space, ed. H. Odishaw, 1
Dmitruk, P., Matthaeus, W. H., Seenu, N., & Brown, M. R. 2003, ApJ, 597, L81
Emslie, A. G. 1981, ApJ, 249, 817
Emslie, A. G. 1983, ApJ, 271, 367
Fletcher, L., & Hudson, H. S. 2008, ApJ, 675, 1645
Fletcher, L., & Warren, H. P. 2003, in Energy Conversion and Particle Acceleration in the Solar Corona, ed. L. Klein, Lecture Notes in Physics (Berlin: Springer Verlag), 612, 58
Fletcher, L., Pollock, J. A., & Potts, H. E. 2004, Sol. Phys., 222, 279
Fletcher, L., Hannah, I. G., Hudson, H. S., & Metcalf, T. R. 2007, ApJ, 656, 1187
Forbes, T. G., & Priest, E. R. 1995, ApJ, 446, 377
Galsgaard, K. 2002, in SOLMAG 2002, Proceedings of the Magnetic Coupling of the Solar Atmosphere Euroconference, ed. H. Sawaya-Lacoste, ESA SP, 505, 269
Galsgaard, K., & Nordlund, Å. 1997, J. Geophys. Res., 102, 231
Hamilton, R. J., & Petrosian, V. 1987, ApJ, 321, 721
Hamilton, R. J., & Petrosian, V. 1992, ApJ, 398, 350
Haug, E. 1997, A&A, 326, 417
Henoux, J. C., & Chambe, G. 1990, J. Quant. Spectrosc. Radiat. Transf., 44, 193
Henoux, J. C., Chambe, G., Smith, D., et al. 1990, ApJS, 73, 303
Horan, D. M. 1971, Sol. Phys., 21, 188
Hudson, H. S. 1972, Sol. Phys., 24, 414
Karlický, M. 2009, ApJ, 690, 189
Kašparová, J., Karlický, M., Kontar, E. P., Schwartz, R. A., & Dennis, B. R. 2005, Sol. Phys., 232, 63
Kašparová, J., Kontar, E. P., & Brown, J. C. 2007, A&A, 466, 705
Kiplinger, A. L., Dennis, B. R., Gordon Emslie, A., Frost, K. J., & Orwig, L. E. 1983, Sol. Phys., 86, 239
Kontar, E. P. 2001, Sol. Phys., 202, 131
Kontar, E. P., & Brown, J. C. 2006, ApJ, 653, L149
Kontar, E. P., & Reid, H. A. S. 2009, ApJ, 695, L140
Kontar, E. P., Hannah, I. G., & MacKinnon, A. L. 2008, A&A, 489, L57
Kontar, E. P., Piana, M., Massone, A. M., Emslie, A. G., & Brown, J. C. 2004, Sol. Phys., 225, 293
Kramers, H. A. 1923, 46, 836
Krucker, S., Kontar, E. P., Christe, S., & Lin, R. P. 2007, ApJ, 663, L109
Krucker, S., Battaglia, M., Cargill, P. J., et al. 2008, A&AR, 16, 155
Krucker, S., Oakley, P. H., & Lin, R. P. 2009, ApJ, 691, 806
Lee, J., & Gary, D. E. 2000, ApJ, 543, 457
Lin, R. P., Dennis, B. R., Hurford, G. J., et al. 2002, Sol. Phys., 210, 3
Lionello, R., Velli, M., Einaudi, G., & Mikic, Z. 1998, ApJ, 494, 840
MacKinnon, A., Vlahos, L., & Vilmer, N. 1992, A&A, 256, 613
MacKinnon, A. L. 2006, Washington DC American Geophysical Union Geophysical Monograph Series, 165, 157
MacKinnon, A. L., & Brown, J. C. 1989, Sol. Phys., 122, 303
Massone, A. M., Emslie, A. G., Kontar, E. P., et al. 2004, ApJ, 613, 1233
Melnik, V. N., Lapshin, V., & Kontar, E. 1999, Sol. Phys., 184, 353
Melrose, D. B., & Dulk, G. A. 1982, ApJ, 259, 844
Miller, J. A., Cargill, P. J., Emslie, A. G., et al. 1997, J. Geophys. Res., 102, 14631
Neidig, D. F. 1989, Sol. Phys., 121, 261
Neupert, W. M. 1968, ApJ, 153, L59+
Piana, M., Massone, A. M., Kontar, E. P., et al. 2003, ApJ, 595, L127
Sakao, T., Kosugi, T., Masuda, S., et al. 1996, Adv. Space Res., 17, 67
Stepanov, A. V., & Tsap, Y. T. 2002, Sol. Phys., 211, 135
Stoiser, S., Brown, J. C., & Veronig, A. M. 2008a, Sol. Phys., 250, 315
Stoiser, S., Brown, J. C., & Veronig, A. M. 2008b, Sol. Phys., 250, 315
Sweet, P. A. 1958, in Electromagnetic Phenomena in Cosmical Physics, ed. B. Lehnert, IAU Symp., 6, 123
Turkmani, R., Vlahos, L., Galsgaard, K., Cargill, P. J., & Isliker, H. 2005, ApJ, 620, L59
Turkmani, R., Cargill, P. J., Galsgaard, K., Vlahos, L., & Isliker, H. 2006, A&A, 449, 749
Veronig, A. M., & Brown, J. C. 2004, ApJ, 603, L117
Veronig, A. M., Brown, J. C., Dennis, B. R., et al. 2005, ApJ, 621, 482
Vlahos, L., & Georgoulis, M. K. 2004, ApJ, 603, L61
Vlahos, L., Isliker, H., & Lepreti, F. 2004, ApJ, 608, 540
Zharkova, V. V., & Gordovskyy, M. 2005, A&A, 432, 1033